

Sign-reversal and non-monotonicity of chirality-related anomalous Hall effect in highly conductive metals

Ryunosuke Terasawa,¹ Masafumi Udagawa,² and Hiroaki Ishizuka¹

¹*Department of Physics, Institute of Science Tokyo, Meguro, Tokyo, 152-8551, Japan*

²*Department of Physics, Gakushuin University, Mejiro, Toshima-ku, Tokyo 171-8588, Japan*

(Dated: February 10, 2025)

The non-monotonic temperature dependence and sign reversal of chirality-related anomalous Hall effect in highly conductive metals are studied. Through the analysis of scattering rate, we find that the non-monotonicity and sign reversal have two major origins: (1) competition between the contribution from short-range and long-range spin correlations and (2) non-monotonic spin correlation in the high-field. The former mechanism gives rise to non-monotonic temperature dependence in a wide range of electron density and, in some cases, a sign reversal of Hall resistivity as the temperature decreases. On the other hand, the latter mechanism is responsible for the sign reversal of Hall conductivity in the high field, which sign reversal generally occurs in magnets with antiferromagnetic interactions. The results demonstrate how the Hall effect reflects local spin correlation and provide insights into the mechanism of non-monotonicity and sign reversal of the anomalous Hall effect by spin chirality.

Introduction — Magnetic materials show rich behaviors in their magnetization process, reflecting their magnetic states and excitations, such as the metamagnetic transitions. Magnetic properties under the external field are often studied through the magnetization curve. In addition, in magnetic metals, transport phenomena also show rich behaviors reflecting the magnetic properties, some of which are difficult to probe by the magnetization curve. One such effect is the anomalous Hall effect (AHE) related to the scalar spin chirality [1–4], which is a distinct mechanism from the ones seen in ferromagnets [5–8]. Later studies have revealed that the AHE is also sensitive to the vector spin chirality [9, 10], coplanar antiferromagnetic order [11, 12], and other non-trivial magnetic states [13–15]. In addition to the AHE, other transport phenomena, such as a resistivity minimum [16, 17], nonreciprocal response [18–20], and spin Hall effect [21–23], are also known to reflect the non-trivial magnetic states. Such studies have been extended to the local spin correlation of fluctuating spins, in which many experiments study chiral spin fluctuation using the transport phenomena [24–32].

Among various transport phenomena, the AHE related to spin chirality has become a popular method for detecting chiral magnetic orders, such as skyrmion crystals. In the AHE, the deviation of anomalous Hall conductivity and magnetization curve is often considered evidence of a chiral magnetic state [3, 33]; the deviation is ascribed to the chirality-related AHE. In experiments, however, the temperature and magnetic field dependence of the chirality-related AHE show rich behaviors. For instance, a sign reversal of chirality-related AHE at low temperatures is known in moderately clean metals [34, 35], which is explained by the competition between intrinsic and skew scattering contributions [36]. Such non-trivial temperature and field dependences were also known in other materials, such as in a highly-conductive metal PdCrO₂ [37–39], in which the skew scattering contribution dominates. However, a

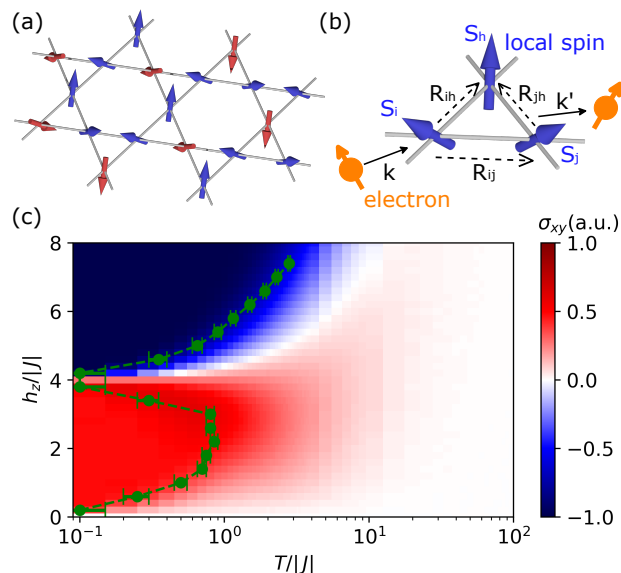


FIG. 1. Ising spin Kondo lattice model and anomalous Hall effect. (a) A schematic of kagomé ice model and (b) skew scattering by multiple spins. (c) Magnetic phase diagram of kagomé ice model and the contour plot of anomalous Hall conductivity at $k_F a = 2.5$. The green dots represent the peak of specific heat.

systematic understanding of such behaviors in the chirality-related AHE is lacking.

To explore the origin of non-trivial temperature dependence of anomalous Hall conductivity in highly conductive metals, we studied the AHE in an Ising-spin Kondo-lattice model on a kagomé lattice called kagomé ice [Fig. 1(a)]; it is a basic model for studying chirality-related AHE [2, 40–42] and relevant to pyrochlore oxides [3, 43] and heterostructures [44]. Using a scattering theory method, we derived a general formula for the anomalous Hall conductivity. This formula is expressed by the scalar spin chirality and the radial wavefunction of electrons at the Fermi

level. We show that the anomalous Hall conductivity exhibits non-monotonic Fermi wavenumber dependence and sign reversals. This behavior reflects the nodes of the Bessel function of the first kind. We also demonstrated that the anomalous Hall conductivity has non-monotonic temperature dependence. This originates from the competition between short- and long-range spin correlations and/or the non-monotonicity of the spin correlations. The results indicate that the non-trivial temperature dependence of AHE can occur in highly conductive metals and clarify their physical origins.

Metallic kagomé ice — Here, we consider two-dimensional free electrons coupled to Ising spins on a kagomé lattice [40, 41]. The Hamiltonian reads

$$H = H_0 + H_K, \quad (1)$$

where,

$$H_0 = \sum_{\mathbf{k}} \epsilon_{\mathbf{k}\mu} c_{\mu}^{\dagger}(\mathbf{k}) c_{\mu}(\mathbf{k}), \quad (2)$$

is the Hamiltonian for free electrons and

$$H_K = J_K \sum_i c_{\mu}^{\dagger}(\mathbf{R}_i) (\mathbf{S}_i \cdot \boldsymbol{\sigma})_{\mu\nu} c_{\nu}(\mathbf{R}_i) \quad (3)$$

is the Kondo coupling between the classical localized spins and itinerant electrons. Here, $c_{\mu}(\mathbf{k})$ [$c_{\mu}^{\dagger}(\mathbf{k})$] is the annihilation (creation) operator of an electron with momentum $\mathbf{k} = (k_x, k_y)$ and spin μ , $k = |\mathbf{k}|$, $\epsilon_{\mathbf{k}\mu} = k^2/2m$ is the eigenenergy of an electron with momentum \mathbf{k} and spin μ , $\boldsymbol{\sigma} = (\sigma_x, \sigma_y, \sigma_z)$ is the vector of the Pauli matrices, $\mathbf{S}_i = (S_i^x, S_i^y, S_i^z)$ is the i th localized moment at position $\mathbf{R}_i = (R_i^x, R_i^y)$. We assume $\mathbf{S}_i \equiv \tau_i \mathbf{d}_i$ to be an Ising spin, where $\tau_i = \pm 1$ and \mathbf{d}_i is the canted easy axis, $(-\frac{2\sqrt{2}}{3}, 0, \frac{1}{3})$, $(\frac{\sqrt{2}}{3}, \sqrt{\frac{2}{3}}, \frac{1}{3})$, and $(\frac{\sqrt{2}}{3}, -\sqrt{\frac{2}{3}}, \frac{1}{3})$ for the three sublattices of the kagomé lattice. In the uniform spin configurations, τ_i takes $(+, +, +)$ for all-in/all-out, $(+, +, -)$ for FM-I, and $(+, -, -)$ for FM-II, as shown in Fig. 3. J_K is the strength of exchange coupling between the itinerant electrons and the localized moment.

Boltzmann theory — To study the AHE arising from the coupling to localized moments, we compute the anomalous Hall conductivity σ_{xy} focusing on the skew scattering contribution [22, 36]. In the Boltzmann theory, skew scattering is described as an asymmetry of scattering rate. The scattering rate $W_{\mathbf{k}\mu \rightarrow \mathbf{k}'\nu}$ is the rate of electron in $|\mathbf{k}\mu\rangle$ state, the μ th eigenstate of H_0 with momentum \mathbf{k} , being scattered to the state $|\mathbf{k}'\nu\rangle$. The skew scattering AHE is related to the difference of $W_{\mathbf{k}\mu \rightarrow \mathbf{k}'\nu}$ and its inverse process $W_{\mathbf{k}'\nu \rightarrow \mathbf{k}\mu}$. To study the asymmetry in the scattering rate, we first define the symmetric $w_{\mathbf{k}\mu \rightarrow \mathbf{k}'\nu}^+$ and antisymmetric $w_{\mathbf{k}\mu \rightarrow \mathbf{k}'\nu}^-$ terms of the scattering rate by $w_{\mathbf{k}\mu \rightarrow \mathbf{k}'\nu}^{\pm} = \frac{1}{2}(W_{\mathbf{k}\mu \rightarrow \mathbf{k}'\nu} \pm W_{\mathbf{k}'\nu \rightarrow \mathbf{k}\mu})$. In this work, we focus on the asymmetric scattering rate $w_{\mathbf{k}\mu \rightarrow \mathbf{k}'\nu}^-$ by the magnetic scattering.

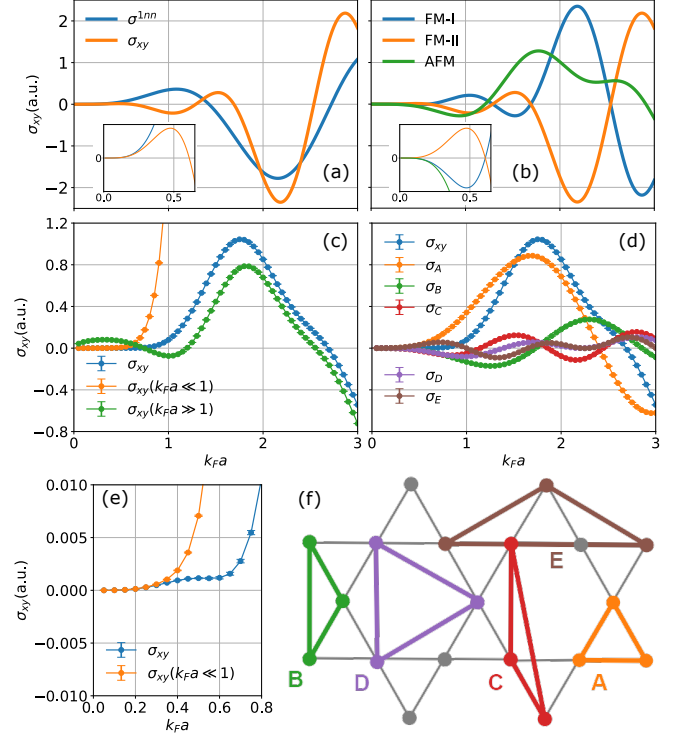


FIG. 2. Fermi wavenumber k_F dependence of the anomalous Hall conductivity in (a) the All-in/All-out state, (b) FM-I, FM-II, and AFM states, and (c) Chiral kagomé ice states; the insets in (a) and (b) show the enlarged view of the small $k_F a$ region for each figure. (d) Contribution of different scattering paths to the Hall conductivity in chiral kagomé ice states. (e) An enlarged view of the small $k_F a$ region of (c). (f) The scattering path involving three spins in kagomé lattice.

The Hall conductivity is calculated by combining the asymmetric scattering rate (see Supplemental Material [45]) with the semiclassical Boltzmann equation [14, 36]. The Hall conductivity σ_{xy} reads

$$\sigma_{xy} = -\frac{\sigma_0 k_F^2}{L^2} \sum_{h,i,j} (\mathbf{S}_h \cdot \mathbf{S}_i \times \mathbf{S}_j) (\hat{R}_{ih} \times \hat{R}_{jh} \cdot \hat{z}) \times J_0(k_F R_{ij}) J_1(k_F R_{ih}) J_1(k_F R_{jh}). \quad (4)$$

Here, $\sigma_0 = \frac{\tau^2 e^2 |m| J_K^3}{2\pi}$, $\mathbf{R}_{ij} = \mathbf{R}_i - \mathbf{R}_j$, L^2 is the area of the system, \hat{z} is the unit vector along the z -axis, $J_n(x)$ ($n = 0, 1$) is the Bessel function of the first kind, k_F is Fermi wavenumber, τ is the relaxation time for symmetric scattering, and e is electric charge.

Hall conductivity — Figure 2 shows the Fermi wavenumber k_F dependence of σ_{xy} considering up to third-nearest-neighbor contributions; Figs. 2(a)-2(d) are for all-in/all-out [Fig. 3(a)], ordered kagomé ice states [see Fig. 3(b)-3(d)], and the chiral kagomé ice state [Fig. 1(a)]. The results show non-monotonic k_F dependence and sign reversal, reflecting the nodes in $J_n(x)$. As evident from Eq. (4), the oscillation occurs in the scale of $k_F \sim$

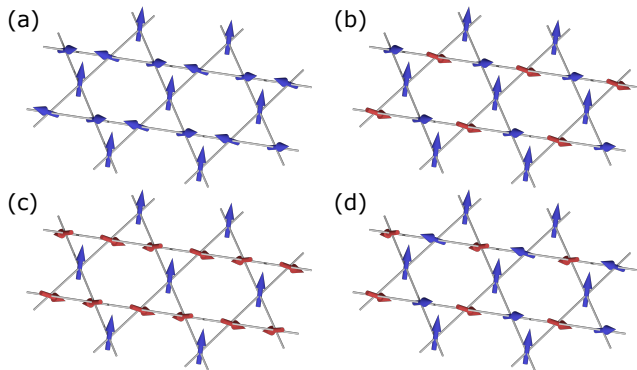


FIG. 3. Schematics of magnetic orders realized in the kagomé ice model: (a) All-in/all-out, (b) FM-I, (c) FM-II, and (d) AFM orders.

$1/R_{ij} \sim 1/a$ where a is the lattice constant. Hence, the Hall conductivity changes sensitively with k_F in a metal where $k_F a$ is comparable to 1.

For a better understanding of the AHE, let us look into the contributions from different terms in Eq. (4). To this end, we classify the terms in σ_{xy} by the scattering process, $\sigma_{xy} = \sigma^{1nn} + \sigma^{2nn}$ where

$$\sigma^{1nn} = \sigma_A + \sigma_B, \quad (5)$$

$$\sigma^{2nn} = \sigma_C + \sigma_D + \sigma_E, \quad (6)$$

with σ_a ($a = A, \dots, E$) being the contribution from the scattering path involving three spins in Fig. 2(f) [45]. The two terms in σ^{1nn} correspond to the contribution from the dominantly nearest-neighbor correlation, and those in σ^{2nn} are the contributions involving the second-nearest-neighbor spin correlation; the terms in σ^{2nn} are limited to C , D , and E as the scalar spin chirality is zero if two of the three spins belong to the same sublattice due to the common anisotropy axis, \mathbf{d}_i . In addition, when we consider the third nearest neighbor spins, the scalar chirality always vanishes because the spins forming a triangle containing the third nearest neighbor spins always contain two or more spins of the same sublattice. Therefore, there are no contributions involving the third-nearest-neighbor spin correlation. Figure 2(a) shows that the trend of σ_{xy} is well captured by σ^{1nn} for a large $k_F a \gtrsim 1$; similarly, the trend of AHE in the kagomé-ice state is well captured by σ_A as shown in Fig. 2(d). On the other hand, the contribution of σ^{2nn} is comparable to that of σ^{1nn} when $k_F a \lesssim 1$. Reflecting the importance of long-range spin correlation, the results for FM-I and AFM ordering in Fig. 2(b) show different trends, despite the fact that the contribution from σ_A is the same in the two cases.

The relatively large effect of σ^{2nn} in the small $k_F a$ region is understandable from the nature of the Bessel function. In the $k_F a \ll 1$ limit, the Hall conductivity reads

$$\sigma_{xy} = -\frac{\sigma_0 k_F^4}{4L^2} \sum_{h,i,j} (\mathbf{S}_h \cdot \mathbf{S}_i \times \mathbf{S}_j) (\mathbf{R}_{ih} \times \mathbf{R}_{jh} \cdot \hat{\mathbf{z}}), \quad (7)$$

as $J_0(x) \sim 1$ and $J_1(x) \sim \frac{x}{2}$ when $x \ll 1$. The equation shows that, in the small $k_F a$ limit, the contribution from each process is proportional to the area covered by the three spins, $\mathbf{R}_{ih} \times \mathbf{R}_{jh} \cdot \hat{\mathbf{z}}$. Therefore, the contribution from the further neighbor spins may take over σ_A if a long-range spin correlation develops at low temperatures.

The anomalous Hall conductivity in the $k_F a \lesssim 0.4$ region is well reproduced by further expanding $J_n(x)$ up to $\mathcal{O}(x^4)$, $J_0(x) \sim 1 - \frac{x^2}{4} + \frac{x^4}{64}$ and $J_1(x) \sim \frac{x}{2} - \frac{x^3}{16}$, as shown in Fig. 2(e). The narrow window of $k_F a$ the small $k_F a$ expansion being valid partly comes from the large R_{ij} in σ^{2nn} . Hence, at a high temperature where the spin correlation ξ is limited to $\xi \lesssim a$, the small $k_F a$ expansion might be valid in a wider range of $k_F a$. However, the region of validity of the approximation is limited in a locally correlated phase, such as in the kagomé ice state [Fig. 2(c)].

On the other hand, the relatively small contribution from σ^{2nn} in the $k_F a \gtrsim 1$ region is understandable from the asymptotic expansion. As shown in Fig. 2(c), the oscillating behavior of Hall conductivity at $k_F a \gtrsim 1$ is well reproduced by the asymptotic expansion of Bessel function about $x \rightarrow \infty$. The asymptotic form of Bessel functions reads $J_0(x) \sim \sqrt{\frac{2}{\pi x}} \cos(x - \frac{\pi}{4})$ and $J_1(x) \sim \sqrt{\frac{2}{\pi x}} \cos(x - \frac{3\pi}{4})$ for $x \gg 1$ [46]. Therefore, the contribution from processes involving further-neighbor spins is suppressed by $R^{-3/2}$ where R is the typical distance between the three spins.

Monte Carlo simulation — To study how the different contributions are reflected in the temperature dependence, we calculated the temperature and magnetic field dependence of spin correlation using a Monte Carlo simulation. To this end, we consider an effective Ising spin model on kagomé lattice,

$$H_S = -J \sum_{\langle i,j \rangle} \tau_i \tau_j - h_z \sum_i \tau_i, \quad (8)$$

where $J < 0$ is the nearest-neighbor exchange interaction and h_z is the magnetic field. This model corresponds to the kagomé ice model with ferromagnetic nearest-neighbor exchange interaction of $-3J$ between canted Ising spins, and the magnetic field $3h_z$ perpendicular to the plane.

Under the ambient magnetic field $|h_z/J| < 4$, the low-temperature state of this model is a locally correlated disorder state [47–49]. At $h_z = 0$, any spin configurations with all triangles in the two-up-one-down or one-up-two-down state are degenerate; it is a classical spin liquid state. Under a weak magnetic field $0 < h_z < 4|J|$, on the other hand, the magnetic field partially lifts the macroscopic degeneracy at $h_z = 0$ as shown in Fig. 4(a). However, the spin configurations with all triangles in the two-up-one-down state are degenerate; this is the chiral kagomé ice (CKI) state [Fig. 1(a)]. The ground state is the all-in/all-out (AIAO) state [Fig. 3(a)] for $h_z > 4|J|$ as in Fig. 4(b).

The temperature and magnetic field dependence of AHE is shown in Fig. 1(c). For $k_F a = 2.5$, the sign of the Hall

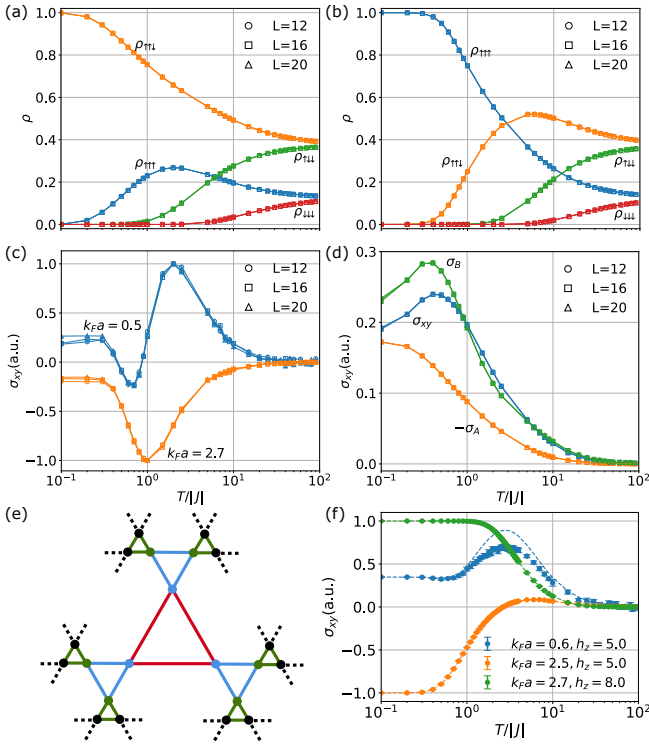


FIG. 4. Monte Carlo simulation of the kagomé ice model under the perpendicular magnetic field. The temperature dependence of the population of triangles with all-up ($\rho_{\uparrow\uparrow\uparrow}$), two-up-one-down ($\rho_{\uparrow\uparrow\downarrow}$), one-up-two-down ($\rho_{\uparrow\downarrow\downarrow}$), all-down ($\rho_{\downarrow\downarrow\downarrow}$) (a) at $h_z = 3.5$ and (b) at $h_z = 5.0$. The temperature dependence of anomalous Hall conductivity (c) at $h_z = 2.0$, $k_F a = 0.5, 2.7$ and (d) at $h_z = 3.4$, $k_F a = 2.5$. (e) A schematic of the Husimi tree. (f) The dots are the results of Monte Carlo simulations, and the dashed lines are the results of the Husimi tree. The simulation was performed with a system of $N = 3 \times 20^2$ sites, using 10^8 Monte Carlo steps each for equilibration and measurement.

conductivity is positive in the CKI state and negative in the AIAO state at low temperatures. It is consistent with the strong coupling theory [40] and that observed in an experiment [44]. However, in general, the magnetic field and the temperature dependence show different behaviors depending on k_F , which cannot be explained by the temperature dependence of spin chirality for the smallest triangles A . Moreover, the temperature dependence of σ_{xy} is often non-monotonic with the temperature as shown in Fig. 4(c). In the last, we note that the sign of σ_{xy} for $k_F a = 2.5$ reflects the scalar spin chirality of triangle B , not A , as shown in Fig. 4(d). The result illustrates the importance of considering the contributions from further-neighbor spin correlation.

Non-monotonicity at low magnetic fields — To understand the origin of the non-monotonic temperature dependence in Figs. 4(c) and 4(d), we plotted $\sigma^{2nn}/\sigma^{1nn}$ with respect to the k_F and magnetic field in Fig. 5(a). The non-monotonic temperature dependence at low magnetic fields, including sign reversal of σ_{xy} in some cases (see Supple-

mental Material [45]), occurs in $k_F a \lesssim 1$ and $k_F a \gtrsim 2$, the k_F at which $\sigma^{2nn}/\sigma^{1nn}$ is mostly negative. The agreement implies that the non-monotonicity is a consequence of the competition between σ^{1nn} and σ^{2nn} . The spin chirality of the triangles that contribute to σ_{xy} shows different temperature dependences; often $\sigma^{1nn} \gg \sigma^{2nn}$ at high temperatures and large $k_F a$. In such a case, the sign of AHE at high temperatures reflects the sign of σ^{1nn} . However, once σ^{2nn} starts to increase at low temperatures, the increase induces non-monotonic temperature dependence. Consequently, the non-monotonic temperature dependence appears when the contribution from the further-neighbor spin correlation is large and $\sigma^{2nn}/\sigma^{1nn} < 0$.

The non-monotonic temperature dependence of χ_B in $0 \lesssim h_z \lesssim 2|J|$ is also attributed to a similar competition between short- and long-range two-spin correlations in the two scattering paths in B [Fig. 5(b)]. We note that the spin correlation of the spin-ice-like states is well described by an effective Gaussian theory [50]. In the Gaussian theory, the three-spin correlation is given as the sum of $\langle \tau_i \tau_j \tau_k \rangle$, where i, j , and k are the indices of three spins on a triangle; at high temperatures, the same conclusion derives from the high-temperature expansion. For triangles like B , in which the distance between spins differs depending on spin pairs, long-range correlations decay faster than short-range ones, as shown in Fig. 5(b). Using the Husimi tree, we find that the nearest-neighbor spin correlation is $\langle \tau_i \tau_j \rangle_1 = \beta J$ and second-nearest-neighbor spin correlation $\langle \tau_i \tau_j \rangle_2 = \beta^2 (J^2 + h^2)$ [45]. As $\langle \tau_i \tau_j \rangle_1 < 0$ and $\langle \tau_i \tau_j \rangle_2 > 0$ when $J < 0$, χ_B becomes non-monotonic at low temperatures in which long-range correlation develops. The non-monotonicity of χ_B is reflected in σ_{xy} near $k_F a = 2.5$ where the influence of χ_B becomes relatively large compared to σ_A , as shown in Fig. 4(d).

Finally, we note that the non-monotonic temperature dependence of magnetization $\langle \tau_i \rangle$ contributes to the non-monotonicity of σ_{xy} near $h = 4|J|$. As shown in Fig. 5(c), a non-monotonic temperature dependence of $\langle \tau_i \rangle$ is often seen in the range $2|J| \lesssim h_z \lesssim 4|J|$. It is likely related to the fact that the lowest excited state is the all-up state for $2|J| \lesssim h_z \lesssim 4|J|$. Calculating the magnetization at low temperatures using the Husimi tree [Fig. 4(e)], which is known to be exactly solvable [51, 52], we find

$$\langle \tau_i \rangle = \frac{1}{3} + \frac{2\sqrt{2}}{9}u - \frac{\sqrt{2}}{3}d - \frac{2}{9}l, \quad (9)$$

where $u = e^{\beta(4J+h_z)}$, $d = e^{-\beta h_z}$, $l = e^{\beta(4J-2h_z)}$ [45]. This equation indicates that $\langle \tau_i \rangle$ becomes non-monotonic at low temperatures when $u > d$, i.e., in the range $2|J| \lesssim h_z \lesssim 4|J|$. Such non-monotonicity of magnetization also takes part in the non-monotonic temperature dependence near $h = 4|J|$.

Non-monotonicity at high magnetic fields — On the other hand, the sign reversal of σ_{xy} at high fields $h > 4|J|$ [see Fig. 1(c)] cannot be explained by the competition of

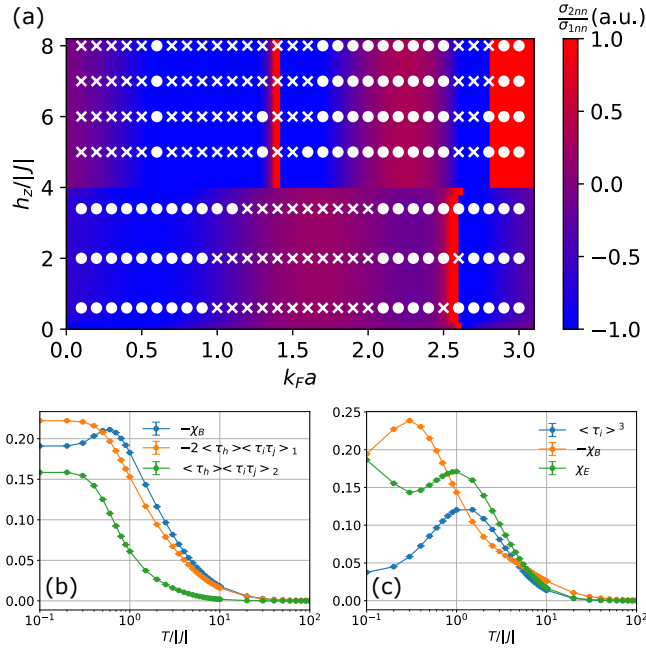


FIG. 5. (a) The k_F and h_z dependence of $\sigma_{2nn}/\sigma_{1nn}$ at $T = 0$. The $\circ(\times)$ denotes that σ_{xy} behaves non-monotonically (monotonically) as the temperature changes at the parameter. T dependence of (b) χ_B , $\langle \tau_h \rangle \langle \tau_i \tau_j \rangle_1$, $\langle \tau_h \rangle \langle \tau_i \tau_j \rangle_2$ at $h_z = 1.5$ and (c) χ_B , χ_E , $\langle \tau_i \rangle^3$ at $h_z = 3.5$. The simulation was performed with a system of $N = 3 \times 20^2$ sites, using 10^8 Monte Carlo steps each for equilibration and measurement.

σ^{1nn} and σ^{2nn} as inferred from Fig. 5(a). For a better understanding of the origin of non-monotonicity at high magnetic fields [Fig. 4(f)], we calculate the three-spin correlation with high-temperature expansion. The thermal average reads

$$\langle \tau_i \rangle = \beta h_z (1 + 4\beta J), \quad (10)$$

$$\langle \tau_i \tau_j \rangle = (\beta h_z)^2 + \beta J, \quad (11)$$

$$\langle \tau_i \tau_j \tau_k \rangle = (\beta h_z)^3 + 3\beta^2 h_z J, \quad (12)$$

where $\langle O \rangle$ represents the thermal average of O [45]. Equation (12) shows that the sign of chirality changes at $T = -h_z^2/3J$ when $J < 0$. As implied from the derivation, which uses the fact that the spins are of Ising type and the exchange interaction is antiferromagnetic, the sign reversal of $\langle \tau_i \tau_j \tau_k \rangle$ is a general feature of antiferromagnetic Ising models.

Summary — In this paper, we studied the temperature dependence of AHE induced by a skew scattering mechanism in a two-dimensional free electron coupled to Ising spins on a kagomé lattice. Using a scattering theory method, we derived a general formula for the anomalous Hall conductivity expressed by a combination of the scalar spin chirality and the Bessel functions of the first kind. We found that the anomalous Hall conductivity exhibits non-monotonic Fermi wavenumber dependence and

sign reversal, reflecting the radial wavelength of electric wavefunctions at the Fermi level. Depending on the value of the Fermi wavenumber and magnetic field, the temperature dependence of Hall conductivity varies [Fig. 5(a)]. At low magnetic fields ($0 \lesssim h_z \lesssim 4|J|$), non-monotonic behavior caused by the competition between σ^{1nn} and σ^{2nn} and/or the non-monotonicity of spin correlation is observed around $k_F a \lesssim 1$ and $k_F a \gtrsim 2$. At high magnetic fields ($h_z \gtrsim 4|J|$), a sign reversal of σ_{xy} is observed at $k_F a \gtrsim 1.7$, reflecting the sign change of chirality at high temperatures. These results demonstrate the non-trivial temperature dependence of chirality-related AHE by skew scattering, which should dominate the AHE in highly-conductive metals.

We are grateful to J. Fujii for providing Python scripts for analyzing the Monte Carlo results. This work is supported by JSPS KAKENHI (Grant Numbers JP19K14649, JP23K03275, JP20H05655, JP22H01147, JP23K22418) and JST PRESTO (Grant No. JPMJPR2452).

-
- [1] J. Ye, Y. B. Kim, A. J. Millis, B. I. Shraiman, P. Majumdar, and Z. Tešanović, “Berry phase theory of the anomalous Hall effect: Application to colossal magnetoresistance manganites,” *Phys. Rev. Lett.* **83**, 3737 (1999).
 - [2] K. Ohgushi, S. Murakami, and N. Nagaosa, “Spin anisotropy and quantum Hall effect in the kagomé lattice: Chiral spin state based on a ferromagnet,” *Phys. Rev. B* **62**, R6065 (2000).
 - [3] Y. Taguchi, Y. Oohara, H. Yoshizawa, N. Nagaosa, and Y. Tokura, “Spin chirality, Berry phase, and anomalous Hall effect in a frustrated ferromagnet,” *Science* **291**, 2573 (2001).
 - [4] G. Tatara and H. Kawamura, “Chirality-driven anomalous Hall effect in weak coupling regime,” *J. Phys. Soc. Jpn.* **71**, 2613 (2002).
 - [5] E. H. Hall, “XVIII. on the “rotational coefficient” in nickel and cobalt,” *Philos. Mag. Ser. 5* **12**, 157 (1881).
 - [6] Robert Karplus and J. M. Luttinger, “Hall effect in ferromagnetics,” *Phys. Rev.* **95**, 1154 (1954).
 - [7] J. Smit, “The spontaneous Hall effect in ferromagnetics ii,” *Physica* **24**, 39 (1958).
 - [8] L. Berger, “Side-jump mechanism for the Hall effect of ferromagnets,” *Phys. Rev. B* **2**, 4559 (1970).
 - [9] H. Ishizuka and N. Nagaosa, “Impurity-induced vector spin chirality and anomalous Hall effect in ferromagnetic metals,” *New J. Phys.* **20**, 123027 (2018).
 - [10] D. Zhang, H. Ishizuka, N. Lu, Y. Wang, N. Nagaosa, P. Yu, and Q.-K. Xue, “Anomalous Hall effect and spin fluctuations in ionic liquid gated SrCoO₃ thin films,” *Phys. Rev. B* **97**, 184433 (2018).
 - [11] H. Chen, Q. Niu, and A. H. MacDonald, “Anomalous Hall effect arising from noncollinear antiferromagnetism,” *Phys. Rev. Lett.* **112**, 017205 (2014).
 - [12] F. R. Lux, F. Freimuth, S. Blügel, and Y. Mokrousov, “Chiral Hall effect in noncollinear magnets from a cyclic cohomology approach,” *Phys. Rev. Lett.* **124**, 096602 (2020).

- [13] T. Yamaguchi and A. Yamakage, “Theory of magnetic-texture-induced anomalous Hall effect on the surface of topological insulators,” *J. Phys. Soc. Jpn.* **90**, 063703 (2021).
- [14] R. Terasawa and H. Ishizuka, “Anomalous Hall effect by chiral spin textures in the two-dimensional Luttinger model,” *Phys. Rev. B* **109**, L060407 (2024).
- [15] J. Mochida and H. Ishizuka, “Anomalous Hall effect sensitive to magnetic monopoles and skyrmion helicity in spin-orbit coupled systems,” *New J. Phys.* **26**, 063031 (2024).
- [16] M. Udagawa, H. Ishizuka, and Y. Motome, “Non-Kondo mechanism for resistivity minimum in spin ice conduction systems,” *Phys. Rev. Lett.* **108**, 066406 (2012).
- [17] Z. Wang, K. Barros, G.-W. Chern, D. L. Maslov, and C. D. Batista, “Resistivity minimum in highly frustrated itinerant magnets,” *Phys. Rev. Lett.* **117**, 206601 (2016).
- [18] T. Yokouchi, N. Kanazawa, A. Kikkawa, D. Morikawa, K. Shibata, T. Arima, Y. Taguchi, F. Kagawa, and Y. Tokura, “Electrical magnetochiral effect induced by chiral spin fluctuations,” *Nat. Commun.* **8**, 866 (2017).
- [19] R. Aoki, Y. Kousaka, and Y. Togawa, “Anomalous nonreciprocal electrical transport on chiral magnetic order,” *Phys. Rev. Lett.* **122**, 057206 (2019).
- [20] H. Ishizuka and N. Nagaosa, “Anomalous electrical magnetochiral effect by chiral spin-cluster scattering,” *Nat. Commun.* **11**, 2986 (2020).
- [21] H. Ishizuka and Y. Motome, “Spontaneous spatial inversion symmetry breaking and spin Hall effect in a spin-ice double-exchange model,” *Phys. Rev. B* **88**, 100402 (2013).
- [22] H. Ishizuka and N. Nagaosa, “Large anomalous Hall effect and spin Hall effect by spin-cluster scattering in the strong-coupling limit,” *Phys. Rev. B* **103**, 235148 (2021).
- [23] K. Nakazawa, K. Hoshi, J. J. Nakane, J. Ohe, and H. Kohno, “Topological spin Hall effect in antiferromagnets driven by vector Néel chirality,” *Phys. Rev. B* **109**, L241105 (2024).
- [24] Y. Fujishiro, N. Kanazawa, T. Nakajima, X. Z. Yu, K. Ohishi, Y. Kawamura, K. Kakurai, T. Arima, H. Mitamura, A. Miyake, K. Akiba, M. Tokunaga, A. Matsuo, K. Kindo, T. Koretsune, R. Arita, and Y. Tokura, “Topological transitions among skyrmion- and hedgehog-lattice states in cubic chiral magnets,” *Nat. Commun.* **10**, 1059 (2019).
- [25] E. Skoropata, J. Nichols, J. M. Ok, R. V. Chopdekar, E. S. Choi, A. Rastogi, C. Sohn, X. Gao, S. Yoon, T. Farmer, R. D. Desautels, Y. Choi, D. Haskel, J. W. Freeland, S. Okamoto, M. Brahlek, and H. N. Lee, “Interfacial tuning of chiral magnetic interactions for large topological Hall effects in $\text{lamno}_3/\text{sriro}_3$ heterostructures,” *Sci. Adv.* **6**, eaaz3902 (2020).
- [26] S.-Y. Yang, Y. Wang, B. R. Ortiz, D. Liu, J. Gayles, E. Derunova, R. Gonzalez-Hernandez, L. Šmejkal, Y. Chen, S. S. P. Parkin, S. D. Wilson, E. S. Toberer, T. McQueen, and M. N. Ali, “Giant, unconventional anomalous Hall effect in the metallic frustrated magnet candidate, KV_3Sb_5 ,” *Sci. Adv.* **6**, eabb6003 (2020).
- [27] Y. Fujishiro, N. Kanazawa, R. Kurihara, H. Ishizuka, T. Hori, F. S. Yasin, X. Yu, A. Tsukazaki, M. Ichikawa, M. Kawasaki, N. Nagaosa, M. Tokunaga, and Y. Tokura, “Giant anomalous Hall effect from spin-chirality scattering in a chiral magnet,” *Nat. Commun.* **12**, 317 (2021).
- [28] K. K. Kolincio, M. Hirschberger, J. Masell, S. Gao, A. Kikkawa, Y. Taguchi, T.-h. Arima, N. Nagaosa, and Y. Tokura, “Large Hall and nernst responses from thermally induced spin chirality in a spin-trimer ferromagnet,” *Proc. Natl. Acad. Sci. U.S.A.* **118**, e2023588118 (2021).
- [29] M. Raju, A. P. Petrović, A. Yagil, K. S. Denisov, N. K. Duong, B. Göbel, E. Şaşıoğlu, O. M. Auslaender, I. Mertig, I. V. Rozhansky, and C. Panagopoulos, “Colossal topological Hall effect at the transition between isolated and lattice-phase interfacial skyrmions,” *Nat. Commun.* **12**, 2758 (2021).
- [30] M. Uchida, S. Sato, H. Ishizuka, R. Kurihara, T. Nakajima, Y. Nakazawa, M. Ohno, M. Kriener, A. Miyake, K. Ohishi, T. Morikawa, M. S. Bahramy, T. Arima, M. Tokunaga, N. Nagaosa, and M. Kawasaki, “Above-ordering-temperature large anomalous Hall effect in a triangular-lattice magnetic semiconductor,” *Sci. Adv.* **7**, eabl5381 (2021).
- [31] N. Abe, Y. Hano, H. Ishizuka, Y. Kozuka, T. Tadano, Y. Tsujimoto, K. Yamaura, S. Ishiwata, and J. Fujioka, “Large anomalous Hall effect in spin fluctuating devil’s staircase,” *npj Quantum Mater.* **9**, 41 (2024).
- [32] K. Karube, Y. Ōnuki, T. Nakajima, H.-Y. Chen, H. Ishizuka, M. Kimata, T. Ohhara, K. Munakata, T. Nomoto, and R. Arita, “Giant Hall effect in a highly conductive frustrated magnet GdCu_2 ,” *arXiv:2409.17478* (2024).
- [33] A. Neubauer, C. Pfleiderer, B. Binz, A. Rosch, R. Ritz, P. G. Niklowitz, and P. Böni, “Topological Hall effect in the A phase of MnSi ,” *Phys. Rev. Lett.* **102**, 186602 (2009).
- [34] N. Kanazawa, Y. Onose, T. Arima, D. Okuyama, K. Ohoyama, S. Wakimoto, K. Kakurai, S. Ishiwata, and Y. Tokura, “Large topological Hall effect in a short-period helimagnet mng,” *Phys. Rev. Lett.* **106**, 156603 (2011).
- [35] D. A. Mayoh, J. Bouaziz, A. E. Hall, J. B. Staunton, M. R. Lees, and G. Balakrishnan, “Giant topological and planar Hall effect in $\text{Cr}_{1/3}\text{NbS}_2$,” *Phys. Rev. Res.* **4**, 013134 (2022).
- [36] H. Ishizuka and N. Nagaosa, “Spin chirality induced skew scattering and anomalous Hall effect in chiral magnets,” *Sci. Adv.* **4**, eaap9962 (2018).
- [37] H. Takatsu, S. Yonezawa, S. Fujimoto, and Y. Maeno, “Unconventional anomalous Hall effect in the metallic triangular-lattice magnet PdCrO_2 ,” *Phys. Rev. Lett.* **105**, 137201 (2010).
- [38] J. M. Ok, Y. J. Jo, K. Kim, T. Shishidou, E. S. Choi, H.-J. Noh, T. Oguchi, B. I. Min, and J. S. Kim, “Quantum oscillations of the metallic triangular-lattice antiferromagnet PdCrO_2 ,” *Phys. Rev. Lett.* **111**, 176405 (2013).
- [39] H. Jeon, H. Seo, J. Seo, Y. H. Kim, E. S. Choi, Y. Jo, H. N. Lee, J. M. Ok, and J. S. Kim, “Large anomalous Hall conductivity induced by spin chirality fluctuation in an ultra-clean frustrated antiferromagnet PdCrO_2 ,” *Commun. Phys.* **7**, 162 (2024).
- [40] H. Ishizuka and Y. Motome, “Quantum anomalous Hall effect in kagome ice,” *Phys. Rev. B* **87**, 081105 (2013).
- [41] G.-W. Chern, A. Rahmani, I. Martin, and C. D. Batista, “Quantum Hall ice,” *Phys. Rev. B* **90**, 241102 (2014).
- [42] M. Udagawa and R. Moessner, “Anomalous Hall effect from frustration-tuned scalar chirality distribution in $\text{Pr}_2\text{Ir}_2\text{O}_7$,” *Phys. Rev. Lett.* **111**, 036602 (2013).
- [43] Y. Machida, S. Nakatsuji, Y. Maeno, T. Tayama, T. Sakai-ibara, and S. Onoda, “Unconventional anomalous Hall ef-

- fect enhanced by a noncoplanar spin texture in the frustrated Kondo lattice $\text{Pr}_2\text{Ir}_2\text{O}_7$,” *Phys. Rev. Lett.* **98**, 057203 (2007).
- [44] M. Ohno, T. C. Fujita, and M. Kawasaki, “Proximity effect of emergent field from spin ice in an oxide heterostructure,” *Sci. Adv.* **10**, eadk6308 (2024).
- [45] Supplemental material to this manuscript is available at ...
- [46] I. S. Gradshteyn and I. M. Ryzhik, *Table of Integrals, Series, and Products*, 8th ed., edited by D. Zwillinger and V. Moll (Academic Press, Boston, 2015) p. 867.
- [47] M. Udagawa, M. Ogata, and Z. Hiroi, “Exact result of ground-state entropy for Ising pyrochlore magnets under a magnetic field along [111] axis,” *J. Phys. Soc. Jpn.* **71**, 2365 (2002).
- [48] R. Moessner and S. L. Sondhi, “Theory of the [111] magnetization plateau in spin ice,” *Phys. Rev. B* **68**, 064411 (2003).
- [49] M. Udagawa and L. Jaubert, eds., *Spin Ice*, Springer Series in Solid-State Sciences, Vol. 197 (Springer International Publishing, 2021).
- [50] S. V. Isakov, K. Gregor, R. Moessner, and S. L. Sondhi, “Dipolar spin correlations in classical pyrochlore magnets,” *Phys. Rev. Lett.* **93**, 167204 (2004).
- [51] Kōji Husimi, “Note on Mayer’s theory of cluster integrals,” *J. Chem. Phys.* **18**, 682 (1950).
- [52] F. Harary and G. E. Uhlenbeck, “On the number of Husimi trees,” *Proc. Natl. Acad. Sci.* **39**, 315 (1953).